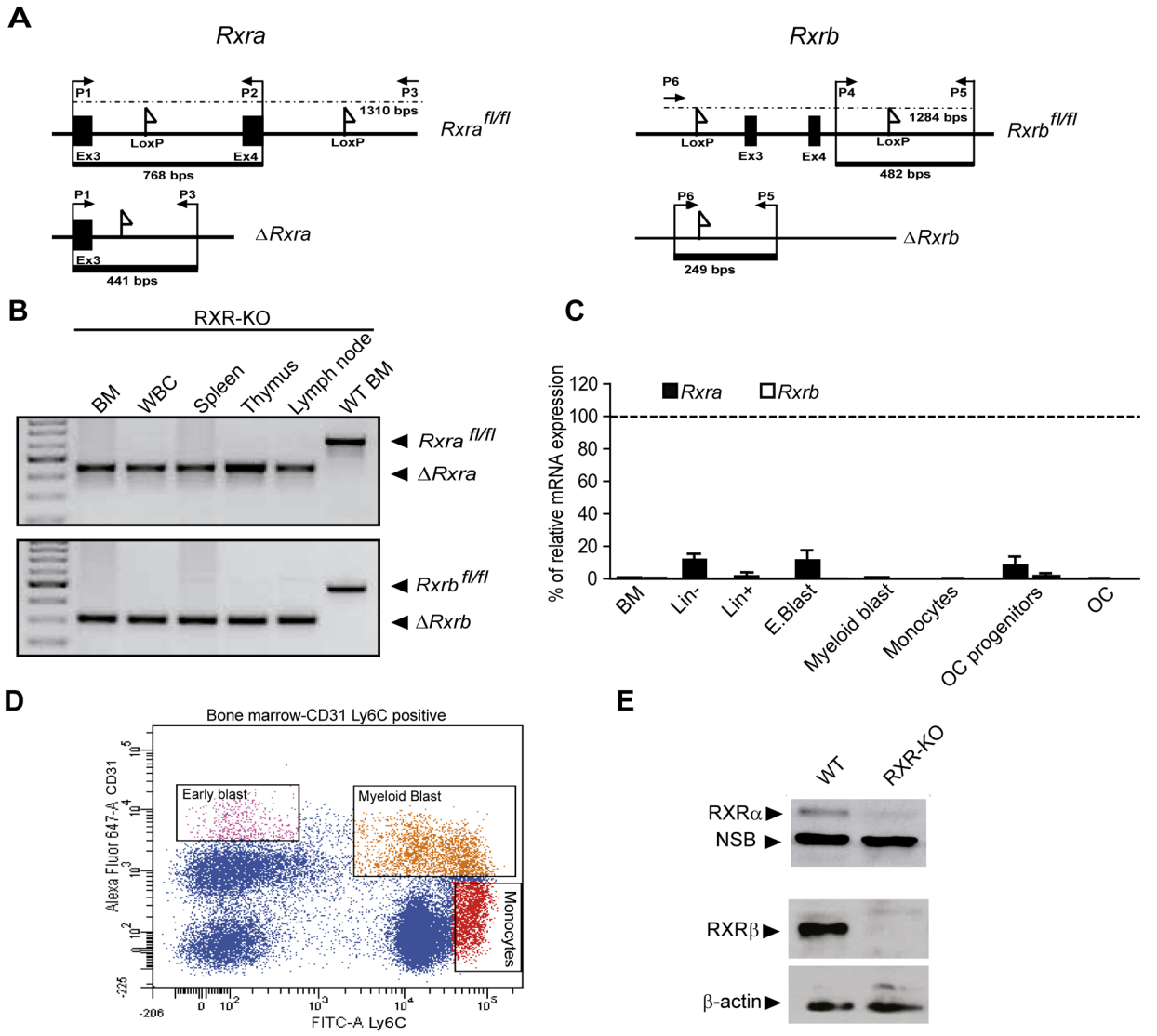

Supplemental Figure 1. Efficiency of Mx1-Cre-mediated loxP recombination in Mx1-Cre RXR-KO mice. (**A**) Layout of *Rxra* and *Rxrb* genes, depicting the intron-exon structures of the targeted genes (*Rxra*$^{fl/fl}$ and *Rxrb*$^{fl/fl}$), the recombined alleles (△*Rxra* and △*Rxrb*), and the positions of the loxP sites. After Cre-mediated recombination, *Rxra* exon 4 and *Rxrb* exons 3 and 4 are deleted. The position of primers used for *Rxra* and *Rxrb* PCR genotyping is shown (P1 to P6). Resulting amplicons and digested band sizes are indicated for each allele. (**B**) PCR analysis of genomic DNA isolated from hematopoietic related tissues of Mx1-Cre^{-} / *Rxrab*$^{fl/fl}$ control mice (WT) and conditionally double-targeted Mx1-Cre^{+} / *Rxrab*$^{fl/fl}$ mice (RXR-KO). Animals were pI:pC-injected at postnatal days 3, 5 and 7. BM, total bone marrow; WBC, white blood cells. (**C**) qPCR analysis of total RNA isolated from different RXR-KO bone marrow cell populations and from in vitro differentiated osteoclast progenitors (OC progenitors) and mature osteoclasts (OC). WT expression levels are considered 100% for each cell population. Data are presented as means ± SEM (n=3 per genotype). BM, total bone marrow; Lin-, lineage- cell fraction; Lin+, lineage+

cell fraction; E. blasts, early blasts. E. blasts, myeloid blasts and monocytes were obtained after labeling total bone marrow cells with CD31 and Ly6C antibodies and sorting the regions represented in (**D**). (**E**) Western blot of total protein isolated from WT and RXR-KO bone marrow cells. NSB, non-specific band. The RXRα and the RXRβ blots are derived from duplicate samples run on 2 separate gels. **B**, **D** and **E** are representative of 3 experiments.

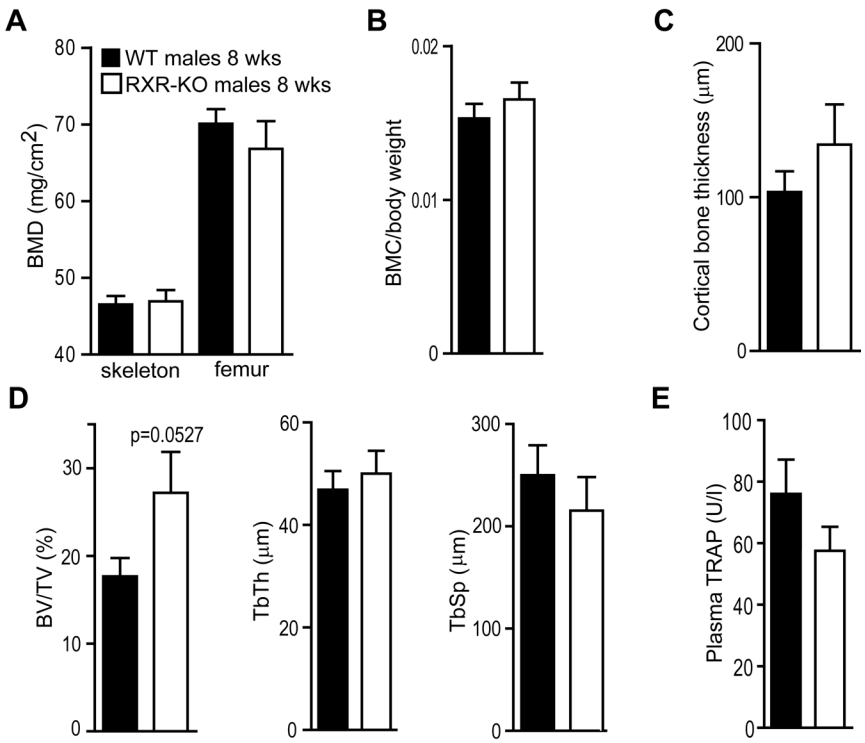

Supplemental Figure 2. Bone phenotype of WT and RXR-KO male mice at 8 weeks of age. (**A**) Bone mineral density (BMD) of the whole skeleton and the femurs. (**B**) Femur bone mineral content (BMC) normalized to body weight (g/g). (**C**) Cortical bone thickness of the femur, measured by μCT at the femoral shaft. (**D**) Histomorphometric parameters of the tibial end of the femur. BV/TV (%), relative bone volume; TbTh, trabecule thickness; TbSp, trabecule separation. (**E**) Plasma TRAP levels. Data are presented as means ± SEM (n=5-6 per genotype). Unpaired 2-tailed Student´s *t*-tests were used for statistical analysis.

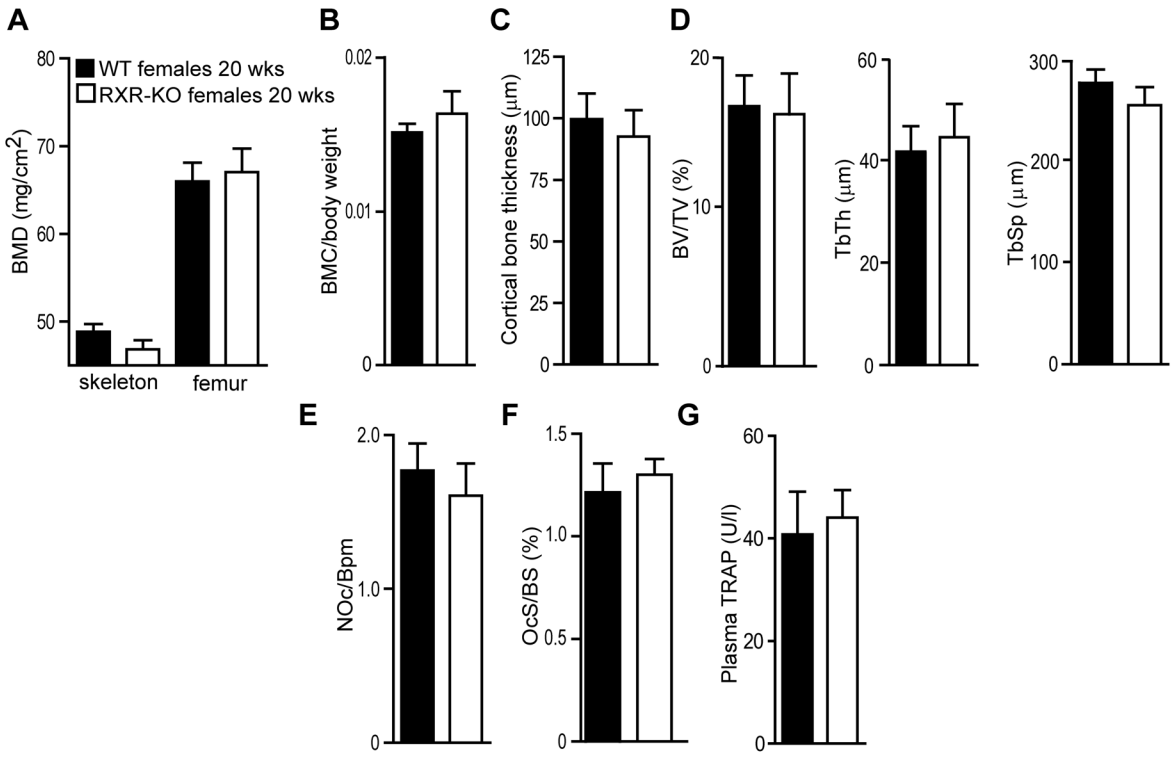

Supplemental Figure 3. Bone phenotype of WT and RXR-KO female mice at 20 weeks of age. (**A**) Bone mineral density (BMD) of the whole skeleton and the femur. (**B**) Bone mineral content (BMC) of the femur normalized to body weight (g/g). (**C**) Cortical bone thickness of the femur, measured with μCT at the femoral shaft. (**D**) Histomorphometric parameters of the tibial end of the femur. BV/TV (%), relative bone volume; TbTh, trabecule thickness; TbSp, trabecule separation. (**E**) Number of osteoclasts normalized to bone perimeter (NOc/Bpm, mm^{-1}). (**F**) Osteoclast surface normalized to bone surface (OCs/BS %). (**G**) Plasma TRAP levels. Data are presented as means ± SEM (n=5-6 per genotype).

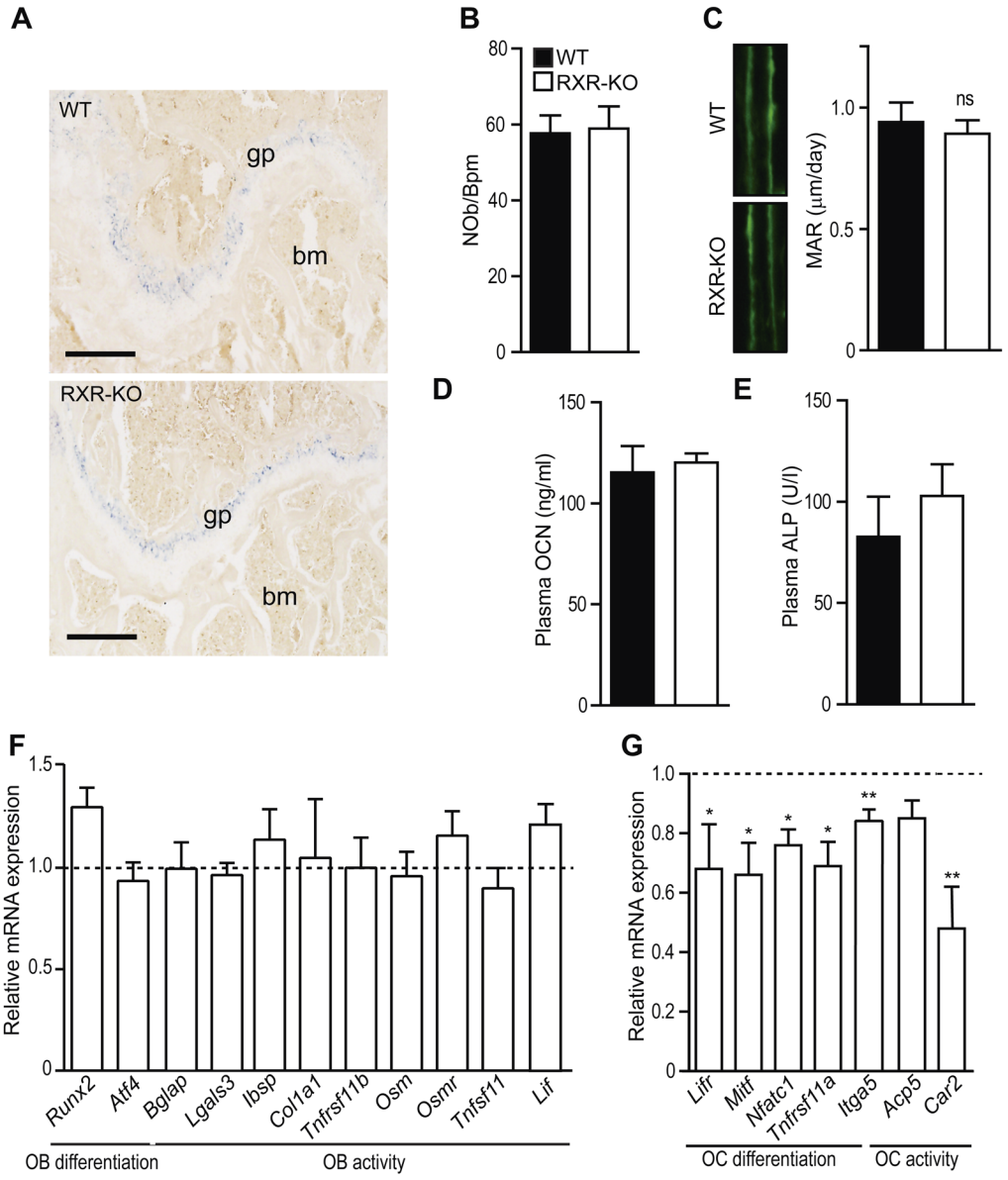

Supplemental Figure 4. Osteoblast and osteoclast differentiation in WT and RXR-KO 20-week-old male mice. (**A**) ALP positive cells (blue) in sections of the tibial end of the femur. gp, growth plate; bm, bone marrow. Scale bars: 120 μm. (**B**) Number of osteoblasts normalized to bone perimeter (NOb/Bpm, mm^{-1}) in the tibial end of the femur. n=6 per genotype. (**C**) Mineral apposition rate (MAR) determined by double calcein labeling; calcein-labeled growth zones are seen in green. n=6 per genotype. (**D-E**) Osteoblast activity markers (osteocalcin [OCN] and alkaline phosphatase [ALP]) were assayed in plasma samples. n=8 per genotype. (**F-G**) Relative transcription of genes involved in osteoblast (OB) and osteoclast (OC) differentiation and activity were determined in mRNA extracted from RXR-KO bone. WT expression levels are considered as 1 for each gene. n=3 per genotype. *Runx2*, Runt-related transcription factor 2; *Atf4*, activating transcription factor 4; *Bglap*, bone gamma carboxyglutamate protein (osteocalcin);

Lgals3, galectin-3; *Ibsp*, bone sialoprotein; *Col1a1*, collagen type I alpha I; *Tnfrsf11b*, tumor necrosis factor receptor superfamily, member 11b (osteoprotegerin); *Osm*, oncostatin M; *Osmr*, oncostatin M receptor; *Tnfsf11*, tumor necrosis factor (ligand) superfamily, member 11 (RANK ligand); *Lif*, leukemia inhibitory factor; *Lifr*, leukemia inhibitory factor receptor; *Mitf*, microphthalmia-associated transcription factor; *Nfatc1*, nuclear factor of activated T-cells, cytoplasmic 1; *Tnfrsf11a*, tumor necrosis factor receptor superfamily, member 11a, NFKB activator (receptor of RANK ligand); *Itga5*, integrin, alpha 5; *Acp5*, tartrate resistant acid phosphatase 5; *Car2*, carbonic anhydrase 2. Data are presented as means ± SEM. ns, non-significant difference. * $P < 0.05$, and ** $P < 0.01$ compared with WT, using unpaired 2-tailed Student´s *t*-test.

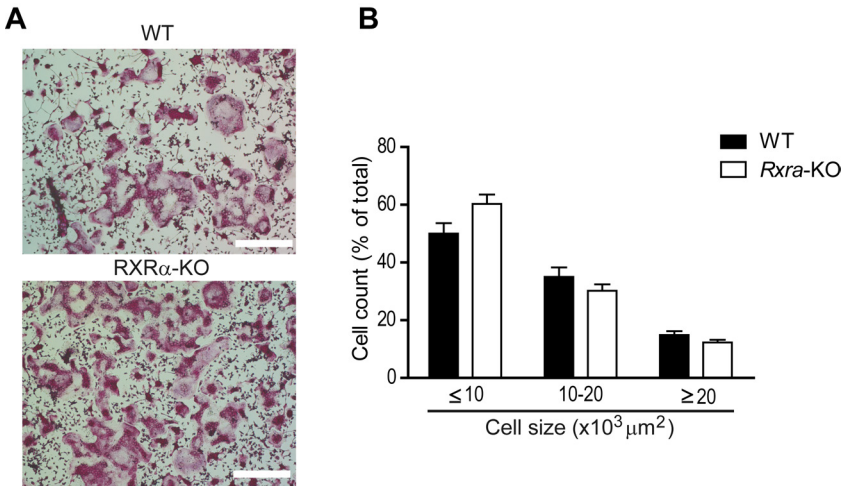

Supplemental Figure 5. Normal osteoclasts in the absence of RXRα (**A**) TRAP-positive osteoclasts differentiated from bone marrow of WT and *Rxra*-KO mice. Scale bars: 100 μm. (**B**) Cell size in the cultured TRAP-positive osteoclasts. Data are presented as means ± SEM of 3 independent experiments done in triplicate.

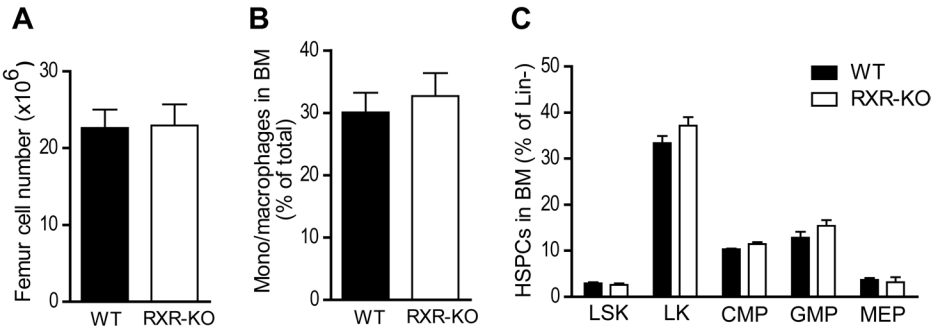

Supplemental Figure 6. Normal numbers of myeloid progenitor cells in 8-week-old RXR-KO mice. (**A**) Total cell number in femur. (**B**) Percentage of monocytes/macrophages in bone marrow (BM). (**C**) Percentage of progenitor cells in bone marrow. Data are presented as means ± SEM (n=6 per genotype). LSK, lineage$^-$, Kit$^+$, Sca-1$^+$ hematopoietic stem cells; LK, lineage$^-$, Kit$^+$, Sca-1$^-$ hematopoietic progenitor cells; CMP, common myeloid progenitors; GMP, granulocyte-macrophage progenitors; MEP, megakaryocyte-erythroid progenitors.

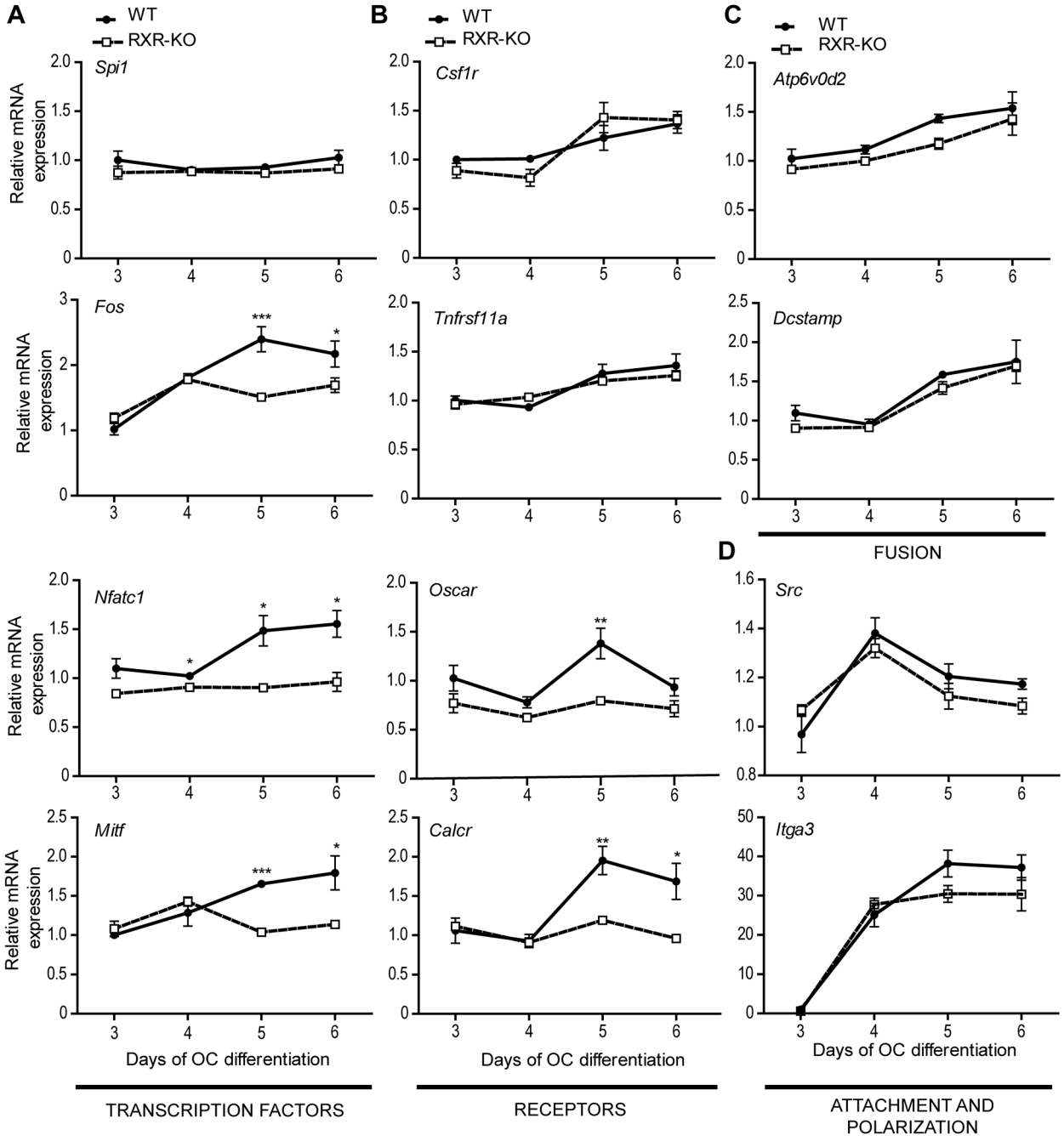

Supplemental Figure 7. Expression of osteoclast differentiation- and function-related genes. Relative mRNA expression of osteoclastogenesis-related transcription factor genes (**A**), receptor genes (**B**), fusion genes (**C**), and attachment and polarization genes (**D**) in the course of in vitro osteoclast differentiation. Data are presented as means ± SEM of a representative independent experiment of 3 done in triplicate. * $P < 0.05$, ** $P < 0.01$, and *** $P < 0.001$ compared with RXR-KO cells on the same day of differentiation, using unpaired 2-tailed Student´s *t*-test. *Spi1*,

spleen focus forming virus proviral integration oncogene (PU.1); *Fos*, c-fos osteosarcoma oncogene; *Nfatc1*, nuclear factor of activated T-cells, cytoplasmic; *Mitf*, microphthalmia-associated transcription factor; *Csf1r*, colony stimulating factor 1 receptor; *Tnfrsf11a*, tumor necrosis factor receptor superfamily, member 11a, NFKB activator; *Oscar*, osteoclast-associated immunoglobulin-like receptor; *Calcr*, calcitonin receptor; *Atp6v0d2*, ATPase, H^+ transporting, lysosomal V0 subunit D2; *Dcstamp*, dendritic cell-specific transmembrane protein; *Src*, proto-oncogene tyrosine-protein kinase; *Itga3*, integrin alpha-3.

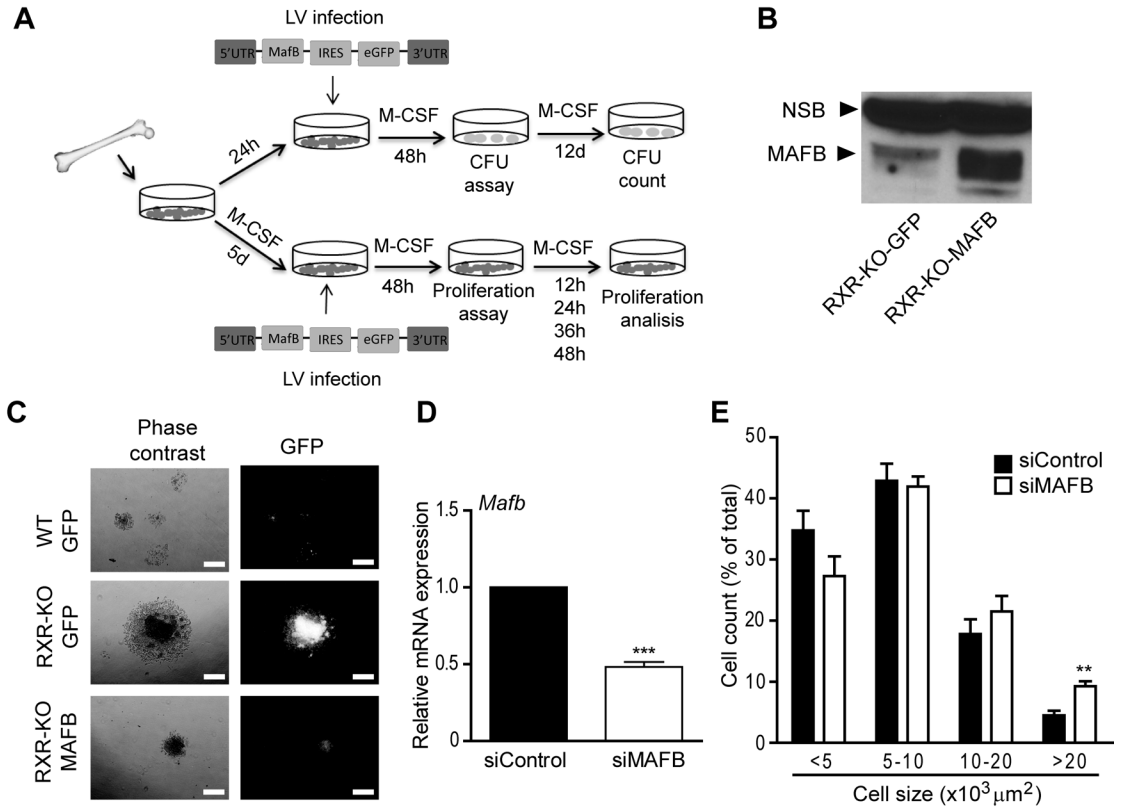

Supplemental Figure 8. MAFB gain and loss of function. (**A**) Experimental outline for lentiviral-mediated expression of MAFB in RXR-KO osteoclast progenitors. (**B**) MAFB protein expression in control- (RXR-KO-GFP) and MAFB- (RXR-KO-MAFB) lentivirus-infected RXR-KO osteoclast progenitors. NSB, non-specific band. (**C**) Representative CFUs in control-lentivirus-infected (WT-GFP and RXR-KO-GFP) and MAFB-lentivirus-infected (RXR-KO-MAFB) bone marrow cell cultures. Scale bars: 100 μm. (**D**-**E**) siRNA assay: (**D**) relative mRNA expression of *Mafb*, and (**E**) cell size analysis of TRAP-positive cells (representative experiment of 3 done in triplicate), after 5 days of differentiation from bone marrow cells transfected with control or *Mafb* siRNAs. Data are presented as means ± SEM (n=3 per group). ** $P < 0.01$ and *** $P < 0.001$ compared with WT using unpaired 2-tailed Student´s *t*-test. **B** and **C** are representative images of 3 experiments.

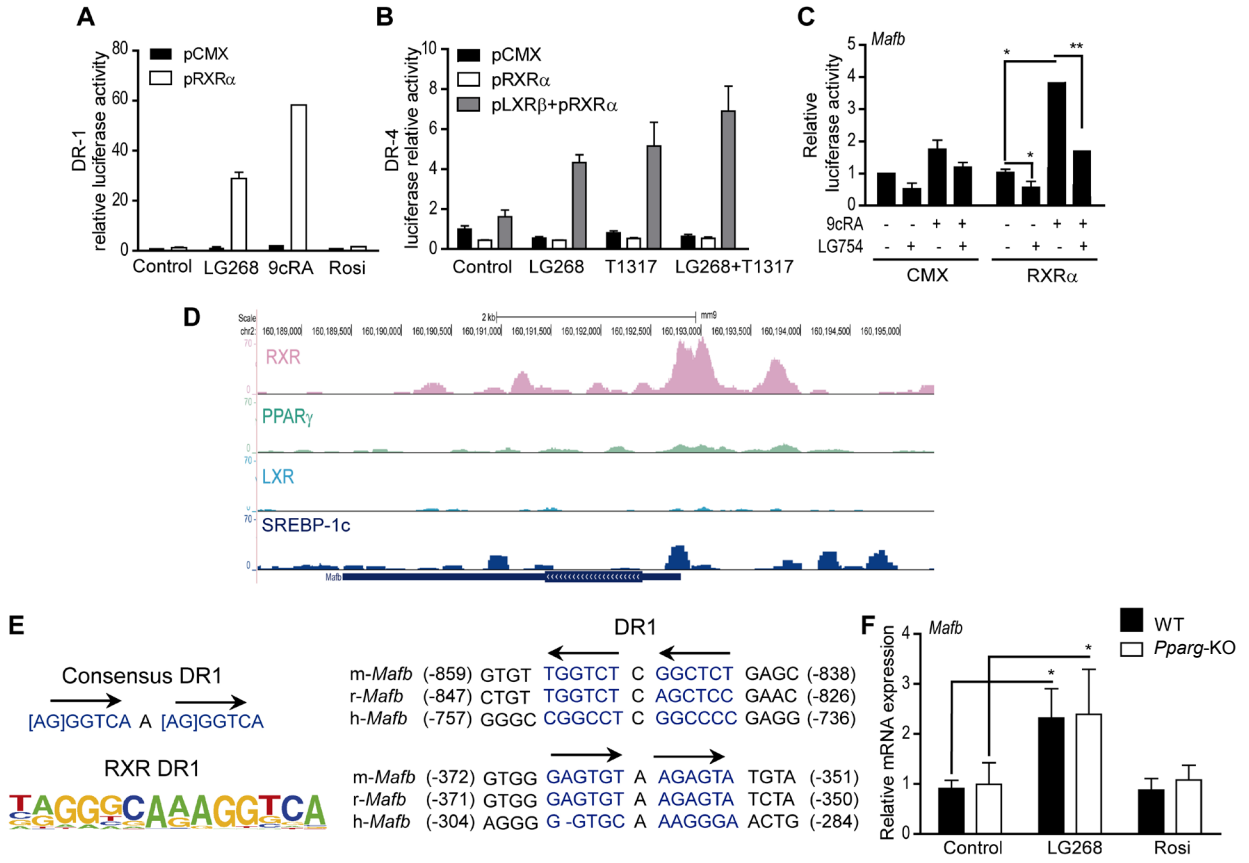

Supplemental Figure 9. *Mafb* expression is regulated by RXR homodimers. (**A** and **B**) Luciferase reporter assays in RAW264.7 cells transfected with RXRα, LXRβ or CMX empty vectors together with a reporter vector containing response elements for RXR or PPAR (DR-1) (**A**) or for LXR (DR-4) (**B**). Data are presented relative to values obtained with vehicle-treated reporters in the absence of RXRα or LXRβ. 9cRA, 9-cis-retinoic acid; Rosi, rosiglitazone. (**C**) Luciferase reporter assay in RAW264.7 cells transfected with RXRα or CMX empty vector together with a reporter vector containing 1.5 kb of the *Mafb* promoter. Data are presented relative to values obtained with the vehicle-treated *Mafb* reporter in the absence of RXRα. (**D**) UCSC Genome Browser (http://genome.ucsc.edu) image depicting RXR, PPARγ, LXR and SREBP-1c ChIP-Seq tags at the *Mafb* gene. (**E**) Alignment of mouse (m), rat (r) and human (h) *Mafb* promoters, showing 2 RXR binding sites, the consensus DR-1 sequence, and the sequence logo for HOMER motif analysis of RXRα-bound regions in macrophages. (**F**) *Mafb* mRNA expression in WT and *Pparg*-KO osteoclast progenitors treated with LG268 or rosiglitazone (Rosi). Data are presented as means ± SEM (n=3 per group). * $P < 0.05$ and ** $P < 0.01$ using paired 2-tailed Student´s *t*-test.

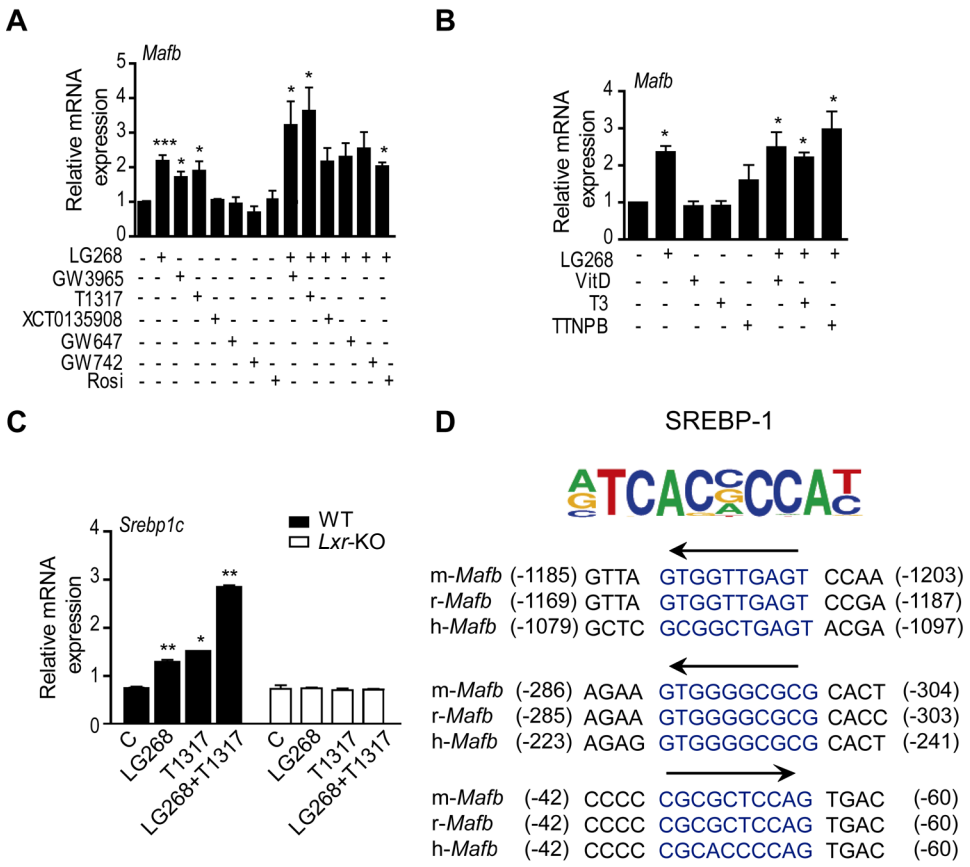

Supplemental Figure 10. RXR/LXR heterodimers regulate *Mafb* expression through SREBP-1c. (**A** and **B**) *Mafb* mRNA expression in WT osteoclast progenitors treated with LG268 and (**A**) ligands for RXR permissive heterodimeric partners (1 μM GW3965 and 1 μM T1317 for LXR, 1 μM XCT0135908 for Nurr1, and 100 nM GW327647, 100 nM GW610742X and 1 μM rosiglitazone for PPARα, PPARβ, and PPARγ respectively), or (**B**) ligands for RXR non-permissive heterodimeric partners (40 nM 1α,25-dihydroxyvitamin D3 (VitD) for VDR, 50 nM triidothyronine (T3) for TR, and 1 μM TTNPB for RAR). * $P < 0.05$ and *** $P < 0.001$ compared with vehicle treated cells. (**C**) *Srebp1c* mRNA expression in WT and *Lxr*-KO osteoclast progenitors treated with LG268, T1317 or a combination of both ligands. (**D**) Alignment of mouse (m), rat (r) and human (h) *Mafb* promoters, showing 3 SREBP-1 binding sites and the sequence logo for HOMER motif analysis of SREBP-1-bound regions in macrophages. Data are presented as means ± SEM (n=3 per group). * $P < 0.05$, ** $P < 0.01$ and *** $P < 0.001$ compared with WT vehicle treated cells (C), using paired 2-tailed Student´s *t*-test.

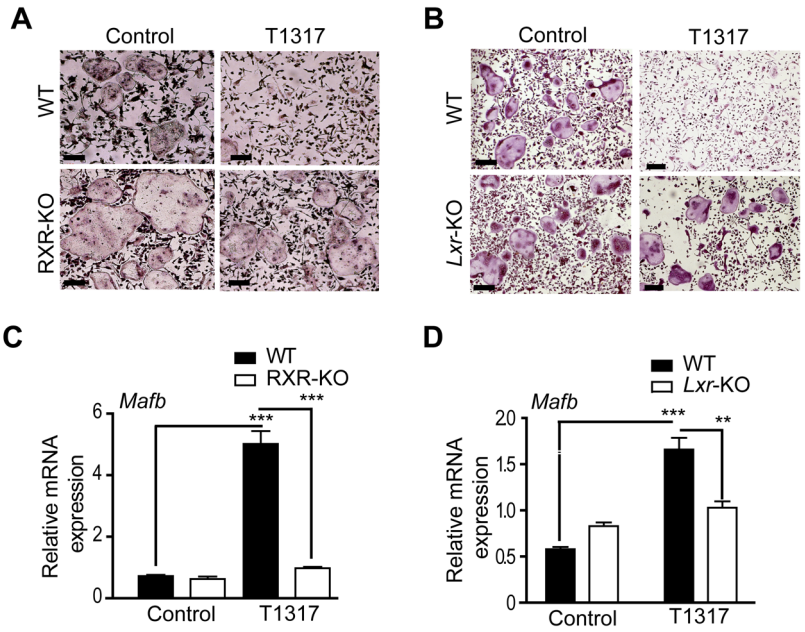

Supplemental Figure 11. Pharmacological activation of RXR/LXR blocks osteoclast differentiation through MAFB. In vitro osteoclast differentiation from WT and RXR-KO (**A** and **C**) or *Lxr*-KO (**B** and **D**) bone marrow cells, treated with vehicle (Control) or T1317: (**A** and **B**) representative mature osteoclasts, identified as multinucleated $TRAP^+$ cells. Scale bars: 100 μm. (**C** and **D**) *Mafb* mRNA expression at day 5 of osteoclast differentiation. Data are presented as means ± SEM (n=3 per group). ** $P < 0.01$ and *** $P < 0.001$, using unpaired 2-tailed Student´s *t*-test. **A** and **B** are representative images of 3 experiments.

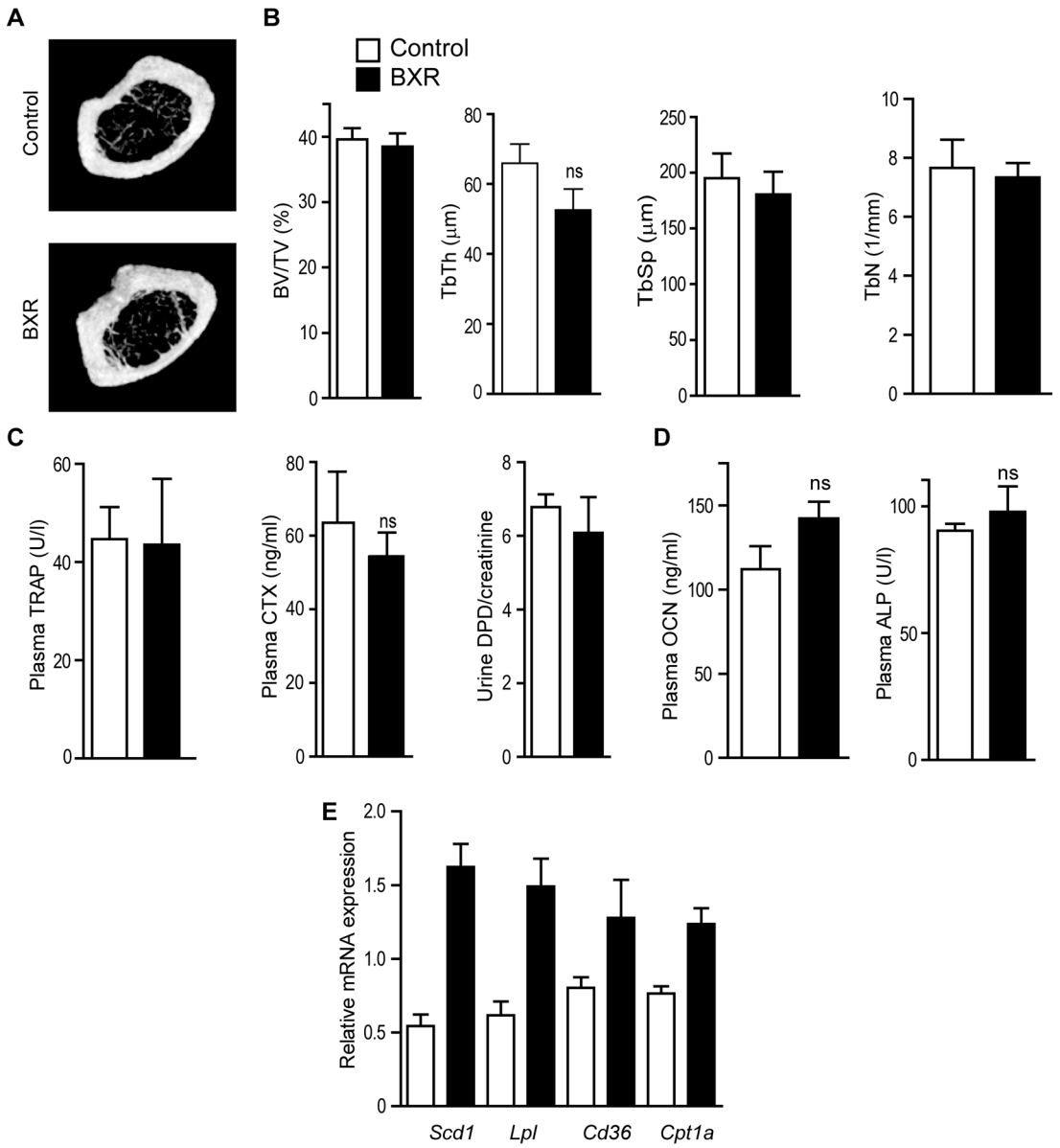

Supplemental Figure 12. Bone parameters of male C57Bl/6 mice after 6 weeks of bexarotene treatment. (**A**) Representative μCT scans of 3 mice per group, showing the distal femur in control and bexarotene (BXR)-treated mice. (**B**) Histomorophometric analysis of the tibial end of the femur. BV/TV (%), relative trabecular bone volume; TbTh, trabecule thickness; TbSp, trabecule separation; TbN, trabecule number. (**C**) Clinical chemistry of osteoclast activity: plasma TRAP and CTX, and urine DPD/creatinine ratio. (**D**) Clinical chemistry of osteoblast activity: plasma OCN and ALP. (**E**) Relative transcription of RXR target genes in the liver in control and BXR treated mice. *Scd1,* stearoyl-Coenzyme A desaturase 1; *Lpl,* lipoprotein lipase; *Cd36,* scavenger receptor class B, member 1; *Cpt1a,* carnitine palmitoyltransferase 1a, liver.

Data are presented as means ± SEM (n=5-6 per genotype). ns, non-significant difference, using unpaired 2-tailed Student´s *t*-test.

Supplemental Table 1: primers used for PCR, qPCR and cDNA amplification.

Assay	Primer name	Sequence (5'-3')
PCR *Rxra* (genotyping)	P1	ACCAAGCACATCTGTGCTATCT
	P2	CAACTGTATACCCCATAGTGTT
	P3	ATGAAACTGCAAGTGGCCTTGA
PCR *Rxrb* (genotyping)	XO141	TCCTCCACTGCACACAGCCC
	WS55	CCGGGAGGGCTGACTTTCATC
qPCR (gene expression)	*Acp5*-F	CAGCAGCCAAGGAGGACTAC
	Acp5-R	ACATAGCCCACACCGTTCTC
	Atf4-F	GAAACCTCATGGGTTCTCCA
	Atf4-R	AGAGCTCATCTGGCATGGTT
	Bglap-F	TGACAAAGCCTTCATGTCCA
	Bglap-R	GTCTAGCCCTCTGCAGGTCA
	Calcr-F	AGTTGCCCTCTTATGAAGGAGAAG
	Calcr-R	GGAGTGTCGTCCCAGCACAT
	Car2-F	ACAGCAACTGCCCAGCAT
	Car2-R	GAGCCCCAGTGAAAGTGAAA
	Cd36-F	GAGCAACTGGTGGATGGTTT
	Cd36-R	GCAGAATCAAGGGAGAGCAC
	Col1a1-F	GCTTCAGTGGTTTGGATGGT
	Col1a1-R	AGGGCGACCTCTCTCACC
	Cpt1a-F	GCCCATGTTGTACAGCTTCC
	Cpt1a-R	AGTGGCCTCACAGACTCCAG
	Csf1r-F	AACACTGGGACCTACCGTTG
	Csf1r-R	GCCATGGCGAGAAGAAGTAG
	Ctsk-F	CAGTCCACAAGATTCTGGGG
	Ctsk-R	GGTTCCTGTTGGGCTTTCAG
	Dcstamp-F	AAAACCCTTGGGCTGTTCTT
	Dcstamp-R	AATCATGGACGACTCCTTGG
	Fos-F	CCATGATGTTCTCGGGTTTC
	Fos-R	TGTCACCGTGGGGATAAAGT
	Ibps-F	GAAAATGGAGACGGCGATAG
	Ibps-R	ACCCGAGAGTGTGGAAAGTG
	Itga5-F	TTCTCCGTGGAGTTTTACCG
	Itga5-R	CACCTGGCTGGCTAGTGTTA
	Itgb3-F	ACCACAGGCAATCAAAAACC
	Itgb3-R	GCGTCAGCACGTGTTTGTAG
	Lgals3-F	GCTTATCCTGGCTCAACTGC
	Lgals3-R	TTCACTGTGCCCATGATTGT
	Lif-F	GTCTTGGCCGCAGGGATTGT
	Lif-R	ACGGCAGTGGGGTTCAGGAC
	Lifr-F	CGGCCAAGAAATCCATAACT
	Lifr-R	AACGAAGTCGGATCATGAGG

qPCR (gene expression)	*Lpl*-F	TTTGGCTCCAGAGTTTGACC
	Lpl-R	TGTGTCTTCAGGGGTCCTTAG
	Mafb-F	AGGACCGCTTCTCTGATGAC
	Mafb-R	GAGCTGCGTCTTCTCGTTCT
	Mitf-F	TTCCCCACAGAGTCTGAAGC
	Mitf-R	CCTTAGCTCGTTGCTGTTCC
	Mmp9-F	CGTCGTGATCCCCACTTACT
	Mmp9-R	AACACACAGGGTTTGCCTTC
	Nfatc1-F	GGTCTTCCGAGTTCACATCC
	Nfatc1-R	CCGATGACTGGGTAGCTGTC
	Oscar-F	CTGCTGGTAACGGATCAGCTCCCCAGA
	Oscar-R	CCAAGGAGCCAGAACCTTCGAAACT
	Osm-F	CCCTCAGTCTCCTCATCCTG
	Osm-R	AGGAAGTGAGGCTTGCTCAG
	Osmr-F	GATGTACCCACTAAGCCGCC
	Osmr-R	GAGGACCGTTGAGGTCAAGC
	Runx2-F	TTACCTACACCCCCGCCAGTC
	Runx2-R	TGCTGGTCTGGAAGGGTCC
	Rxra-flox/out-F	TACAGTTGTGAGGGCTGCAA
	Rxra-flox/out-R	TTCCGCTGTCTCTTGTCGAT
	Rxrb-flox/out-F	ATGTGAAGCCACCGGTCTTA
	Rxrb-flox/out-R	GCTTGAAGAAACCCTTGCAG
	Scd1-F	AGCTGGTGATGTTCCAGAGG
	Scd1-R	ATCGCAAGAAGGTGCTAACG
	Spi1-F	CCCACACCGGCCTCAGT
	Spi1-R	GACAAGGTTTGATAAGGGAAGCA
	Src-F	CTACACCACAGATGCCGATG
	Src-R	CCCCCTTCCCTATTGTCTGT
	Srebp1-F	AGGCCATCGACTACATCCG
	Srebp1-R	ATCCATAGACACATCTGTGCCTC
	Tnfsf11-F	TGTACTTTCGAGCGCAGATG
	Tnfsf11-R	AGGCTTGTTTCATCCTCCTG
	Tnfrsf11a-F	TGCAGCTCAACAAGGATACG
	Tnfrsf11a-R	GAGCTGCAGACCACATCTGA
	Tnfrsf11b-F	TGTTCCGGAAACAGAGAAGC
	Tnfrsf11b-R	CTCTCGGCATTCACTTTGGT
Amplification of *Mafb* cDNA (lentiviral vector)	FWD	GTAAGGATCCATGGCCGCGGAGCTGAG
	REV	GCTGGGATCCTCACAGAAAGAACTCAGG
qPCR (ChIP)	*Igkappa*-F	GCAACTGTCATAGCTACCGTC
	Igkappa-R	GTCTTAGAGGCTTTGGAAACT
	Mafb1-F	CTGAGCTGGGAAGCAAAAAG
	Mafb1-R	TGTGGGACTTTCCTCAGACC

qPCR (ChIP)	*Mafb2*-F	ACTTGGGGTCGCACTTTATG
	Mafb2-R	TCTGTGCACTCAGTGGCTCT
	Mafb3-F	CGAGGGTGGGAGTGTAAAGA
	Mafb3-R	ACCCTCTGAGTCGAGGTTCC
	Mafb4-F	GCAAGCAAGAAAGCCCTAGA
	Mafb4-R	GGGAACGAGTCAGGTCGAG

Supplemental Video 1. Image sequences show motile (1A, 1B) and stationary (2A, 2B) osteoclasts. The motile WT osteoclast develops a predominant leading edge and clear tail as the cell translocates, whereas the RXR-KO osteoclast develops multiple membrane protrusions none of which become a predominant leading edge. The stationary WT osteoclast develops some regions that protrude and others that retract, while the RXR-KO osteoclast protrudes along the whole perimeter of the cells. Acquisition time was 15 min for motile and 30 min for stationary osteoclasts, at one frame/ minute. The image sequences were obtained with a Leica wide field microscope fitted with differential interference contrast objective. Representative of 3 independent experiments.